Engineering with Computers (2016) 32:85–97
DOI 10.1007/s00366-015-0400-7

ORIGINAL ARTICLE

Prediction of seismic slope stability through combination of particle swarm optimization and neural network

Behrouz Gordan · Danial Jahed Armaghani · Mohsen Hajihassani · Masoud Monjezi

Received: 8 September 2014 / Accepted: 31 January 2015 / Published online: 18 February 2015

Abstract One of the main concerns in geotechnical engineering is slope stability prediction during the earthquake. In this study, two intelligent systems namely artificial neural network (ANN) and particle swarm optimization (PSO)–ANN models were developed to predict factor of safety (FOS) of homogeneous slopes. Geostudio program based on limit equilibrium method was utilized to obtain 699 FOS values with different conditions. The most influential factors on FOS such as slope height, gradient, cohesion, friction angle and peak ground acceleration were considered as model inputs in the present study. A series of sensitivity analyses were performed in modeling procedures of both intelligent systems. All 699 datasets were randomly selected to 5 different datasets based on training and testing. Considering some model performance indices, i.e., root mean square error, coefficient of determination (R^2) and value account for (VAF) and using simple ranking method, the best ANN and PSO–ANN models were selected. It was found that the PSO–ANN technique can predict FOS with higher performance capacities compared to ANN. R^2 values of testing datasets equal to 0.915 and 0.986 for ANN and PSO–ANN techniques, respectively, suggest the superiority of the PSO–ANN technique.

Keywords Factor of safety · Limit equilibrium method · Artificial neural network · Particle swarm optimization

B. Gordan (✉) · D. Jahed Armaghani
Department of Geotechnics and Transportation, Faculty of Civil Engineering, Universiti Teknologi Malaysia, 81310 UTM Skudai, Johor, Malaysia
e-mail: bh.gordan@yahoo.com

D. Jahed Armaghani
e-mail: danialarmaghani@yahoo.com

M. Hajihassani
Construction Research Alliance, Universiti Teknologi Malaysia, 81310 UTM Skudai, Johor, Malaysia
e-mail: mohsen_hajihassani@yahoo.com

M. Monjezi
Department of Mining, Tarbiat Modares University, Tehran 14115-143, Iran
e-mail: monjezi@modares.ac.ir

1 Introduction

The design of stabilized slope under earthquake forces is one of the interesting areas in the field of geotechnical engineering. Slope stabilization methods are possible with specific skills, but should involve the comprehensive study for simulation in realistic ways. Moreover, model analysis with high level of accuracy depends on parameters related to subsurface conditions, ground behavior and applied loads. Generally, the main purpose of slope stability is to establish a safe and economic design of the structures such as earth dam, embankment, excavations and landfills. Static analysis is one of the major factors in slope design for artificial slopes. In this regard, the limit equilibrium methods (LEM) have been widely used to compute the factor of safety (FOS). In slope stability analysis, the slice of soil mass above failure surface plays a major role on FOS in which it has been considered as a circular slide line [1, 2], general slide line [3] and inclined slices [4, 5].

Recently, finite element method (FEM) has been utilized based on displacement characteristic to evaluate FOS using the shear strength reduction (SSR) or phi-c reduction technique [6, 7]. In addition, some combined methods based on probabilistic approaches of slope stability analysis and design with an aid of both LEM and FEM methods have been carried out [8]. Several methods have been developed

for this purpose, such as Monte Carlo simulation [9], nonlinear failure statistical method [6], Microsoft Excel-based program [10], geographic information system (GIS) [11, 12], logistic regression approach [13], and artificial intelligent methods [14–16]. From these studies, it was found that all the methods can be utilized for slope stability problems.

Among the mentioned approaches, artificial intelligent techniques such as artificial neural network (ANN), fuzzy inference system (FIS), and neuro-fuzzy (ANFIS) have received the most attention in the field of geotechnical engineering [17–23]. Sakellariou and Ferentinou [24] compared the calculated FOS using standard analytical methods to predicted FOS by neural network analyses. Das et al. [25] developed two ANN models to predict FOS using data based on the study by Sah et al. [26]. In their study, the input parameters considered were slope height, unit weight, cohesion, internal angle of friction, gradient and pore pressure. The ANN results were in good agreement with the real results. Choobbasti et al. [27] considered total and effective stresses, gradient, coefficient of cohesion, internal angle of friction, and horizontal coefficient of earthquake as inputs to predict FOS by ANN. The simulated results were compared with the results from classical LEM to check the validity of ANN model. Finally, they concluded that the ANN results are considerably close to the values calculated by Bishop's method. Samui and Kothari [28] utilized a least square support vector machine (LSSVM) model for analysis of 46 safety factor values. In their study, unit weight (γ), cohesion (c), internal angle of friction (ϕ), slope angle (β), height (H) and pore water pressure coefficient (r_u) were used to predict FOS. For comparison purpose, an ANN was modeled using the same input and output parameters. Correspondingly, the LSSVM model yielded better results in comparison to the ANN model. Moreover, Erzin and Cetin [29] predicted the critical FOS of homogeneous finite slopes using ANN and multiple regression (MR) models. 675 values of FOS obtained from simplified Bishop method were used for prediction purpose. They utilized two different groups of analysis. For the first group (ANN-1 and MR-1), five parameters (unit weight, cohesion, internal friction angle, slope angle, and height) were considered as inputs while for the second group (ANN-2 and MR-2), four parameters (cohesion, internal friction angle, slope angle, and height) were used as inputs to predict FOS. The first group of analysis has shown higher prediction performance compared to the second group.

Artificial neural networks (ANNs), as powerful tools of artificial intelligence, are one of the most dynamic areas of research in advanced and diverse applications of science and engineering. Although ANNs are able to apply all the influential factors to predict the relationship between the input and the output parameters, they still have some limitations: the slow rate of learning and getting trapped in local minima [30]. To overcome these restrictions, use of powerful optimization algorithms is of advantage. Particle swarm optimization (PSO) is a powerful population-based technique for solving continuous and discrete optimization problems [31, 32]. Since PSO is a robust global search algorithm, it can be utilized to determine weights and biases of ANN to improve its performance. In this study, two intelligent systems namely ANN (back-propagation) and hybrid PSO–ANN have been developed to predict FOS obtained from Geostudio program. Eventually, the obtained results of both intelligent systems were evaluated and best ANN and PSO–ANN models of FOS prediction were selected.

2 LEM modeling procedure

To obtain the suitable datasets of FOS analysis, modeling procedure was conducted in several steps. The process consisted of introducing boundary conditions, model dimensions, material properties and seismic motion. Bishop's method utilizing GeoStudio was applied to obtain FOS values in this research.

Many homogenous slopes (in terms of material, $\gamma = 18$ kg/m^3) with various conditions were modeled to obtain FOS in the study. Slopes with heights of 15, 20, 25 and 30 m, and gradients of 20°, 25°, 30° and 35° were designed. All the models were located on the bedrock with respect to the rigid behavior. In addition, the crest width of 8 m was assumed for all the models. Figure 1a shows a symbolic model used in this research. It should be noted that all models were designed in plane strain (2D) condition according to wide valley shape, because the lateral

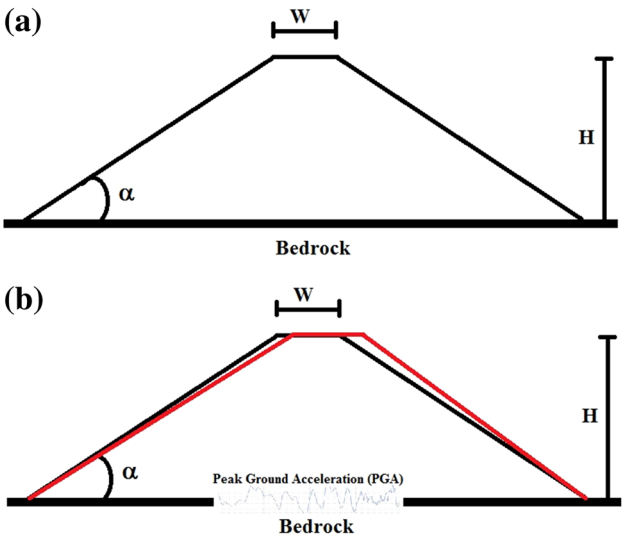

Fig. 1 **a** Model dimensions and **b** dam deformation under earthquake

displacement in embankment can be limited to zero under this condition [33].

The Mohr–Coulomb (MC) failure criterion was considered for the analysis in this study. Cohesions of 20, 30, 40 and 50 kPa and internal friction angles of 20°, 25°, 30°, 35° and 40° were applied in the analyses process. The earthquake motion effect is very important in controlling dam behavior. In terms of scope of this study, the soil density for all models was considered as 18 (kg/m^3). Figure 1b shows the embankment deformation regarding the earthquake accelerator motions. According to Kramer [34], peak ground acceleration (PGA) is a measure of earthquake acceleration on the ground. In this study, the amplitudes of PGA were considered to be 0.1, 0.2, 0.3 and 0.4 g.

As mentioned earlier, FOS values were computed for various slope conditions. Thirty slices were used as slip surfaces for all the slope models. In this study, grid and radius slip surface was utilized to achieve FOS values. Note that, in the grid and radius method, the computed FOS should be located almost in the middle of the grid.

3 PSO–ANN hybridization

3.1 Artificial neural network

Artificial neural network is an information-processing system. In this system, the information is processed by several interconnected simple elements that are known as neurons, positioned in the network's separated layers. The best neural network is the multi-layer perceptron (MLP) that is composed of three separate layers: input, output, and the intermediate or the hidden layers [35]. Difficulty level of the problem determines the number of the hidden layers and neurons [36]. Each neuron of a layer is connected to all the neurons of the next layer, but this connection is not within the same layer. After processing information, the connection links transmit it between the neurons. There is a weight assigned to each link where this weight is multiplied into the transmitted signal.

A neural network performance is dependent on topology or architecture of the network including the number of hidden layer(s) and the number of neurons in the hidden layer(s). The network should be trained with enough input–output patterns that are known as the training pairs [37]. The training is terminated once the error reaches the specified error and the optimum model is then specified. Several algorithms have been recommended for the training purpose of the neural network. Back-propagation (BP) algorithm is the most powerful technique for MLP networks as mentioned by many scholars [38–40]. In feed-forward BP ANNs, artificial neurons are organized by layers and send their signals forward. In this algorithm, based on the difference between the predicted and actual network outputs, the weights of the inter-neuron connections are adjusted [41]. This procedure is known as learning or training. The difference between predicted and actual outputs is known as network error. The obtained error is propagated back through the network and updates the individual weights which is named backward pass. The process is repeated until the error is converged to a defined level such as root mean square error (RMSE) [42].

3.2 Particle swarm optimization

Particle swarm optimization (PSO) developed by Kennedy and Eberhart [43] is a powerful optimization technique inspired by social behavior of bird flocking or fish schooling. In the PSO algorithm, a number of particles are placed in the search space of N-dimensional problem. Each particle represents a potential solution and estimates the objective function at its current position. In this model, particles are flown repetitively through the problem search space. The next location of each particle is determined by combining its current and best position with some random perturbations [44]. Eventually, the swarms move close to the optimum fitness function [45]. In PSO, the position and velocity of the particles are updated based on Eqs. 1 and 2, respectively.

$$X_i^{k+1} = X_i^k + V_i^{k+1} \tag{1}$$

$$V_i^{k+1} = V_i^k + c_1\, r_1 \left(p_{\text{best},i}^k - X_i^k\right) + c_2\, r_2 \left(g_{\text{best}}^k - X_i^k\right) \tag{2}$$

where X_i^k is the N-dimensional vector that represents particle position (i) at iteration (k). V_i represents the velocity of this particle. The velocity vector derives the optimization process by reflecting both the experimental knowledge of the particle and socially shared information from the particle's neighborhood [46]. The best position of the particle is denoted by $p_{\text{best},i}$ and $g_{\text{best},}$ respectively, in Eqs. 3 and 4. In the above equations, r_1 and r_2 are random values in the range of [0,1], and c_1 and c_2 are positive acceleration constants. The fitness function f measures how close the corresponding solution is to the optimum by calculating $p_{\text{best},i}$ and g_{best}. The personal and global best positions at the next iteration are defined as:

$$p_{\text{best},i}^{k+1} = \begin{cases} X_i^{k+1}, f\left(X_i^{k+1}\right) < f\left(p_{\text{best},i}^k\right) \\ P_{\text{best},i}^k, f\left(X_i^{k+1}\right) \geq f\left(p_{\text{best},i}^k\right) \end{cases} \tag{3}$$

$$g_{\text{best}}^k \in \left\{p_{\text{best},0}^k, \ldots, p_{\text{best},n_s}^k\right\} \Big| f\left(g_{\text{best}}^k\right) = \min\left\{f\left(p_{\text{best},0}^k\right), \ldots, f\left(p_{\text{best},n_s}^k\right)\right\} \tag{4}$$

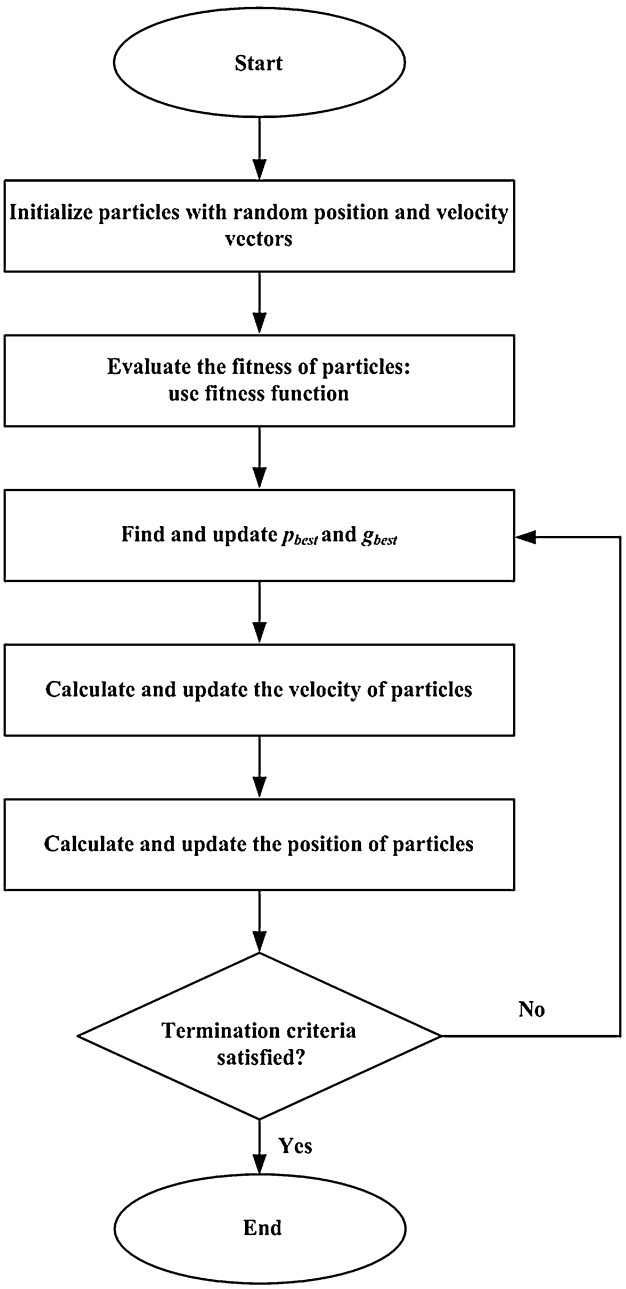

Fig. 2 Flowchart depicting the general PSO algorithm

where n_s denotes the total number of particles in the swarm. The particles continue to move in the search space, with their position being updated at each iteration until the stopping condition is met. Figure 2 demonstrates the workflow of PSO algorithm.

Compared to other evolutionary algorithms, PSO is a stochastic gradient-free search algorithm with reduced memory requirement, easier to be applied and computationally effective [47]. However, the major drawback of PSO is the slow fine tuning of the solution [47] and its inefficiency in searching for local optima [48]. Indeed, PSO is a global algorithm with strong ability to find global optimum, but the search process around the global optimum is very slow in this approach [49]. Therefore, combining the PSO algorithm with a strong local search technique leads to better search result.

3.3 Combination of PSO–ANN algorithm

Many attempts have been made to increase the ANN performance by means of optimization algorithms due to the fact that optimum search development of conventional ANNs might fail and return unsatisfied solution [50]. Some studies have been performed to identify the PSO ability as a training algorithm for a number of ANN architectures. Several researchers have demonstrated the capability of PSO in training ANNs and showed that the PSO is an effective alternative to train ANNs [51–54]. Besides, some other attempts have been made to utilize other optimization approaches in training ANNs, e.g., genetic algorithm and ant colony optimization techniques [55, 56]. Nevertheless, it has been found that ANNs trained by PSO provide more accurate results in comparison to other learning algorithms [50].

A set of weights and biases are determined in ANN training to minimize objective functions such as RMSE. In the ANN-PSO method, definition of fitness function is required to generate models. RMSE can be employed as a fitness function in this method. There are one global minimum and a number of local minima in the minimization problems. ANN searches solution in the local region due to its inherent property and, therefore, normally gets trapped in a local minimum. PSO has a competent capability to seek the entire search space to find the global minimum and continues searching around it. Hence, a hybrid PSO–ANN model encompasses the properties of both PSO and ANN in which PSO looks for the global minimum in the search space and ANN utilizes the global minimum to find the best results.

4 Intelligent systems in predicting FOS

Two intelligent systems namely ANN and PSO–ANN were developed to predict FOS obtained from Geostudio software. In this regard, 699 homogenous slopes with their most influential parameters on FOS were modeled. Then, FOS values were determined for each slope. Selecting the input parameters is the most important step for developing a predictive model. To develop comprehensive and accurate models, the most influential parameters on FOS should be selected. Therefore, the most influential parameters on FOS including slope height (H), gradient (α), cohesion (C), friction angle (ϕ) and PGA were selected as model inputs.

Table 1 Statistical information of input and output parameters

Parameter	Category	Symbol	Min	Max	Average	Std. deviation	Variance
Slope height (m)	Input	H	15	30	22.32	5.6	31.37
Gradient (°)	Input	α	20	35	25.16	5.13	26.37
Cohesion (kg/cm^2)	Input	C	20	50	35.28	11.18	124.96
Friction angle (°)	Input	ϕ	20	40	34.07	5.88	34.59
Peak ground acceleration (m/s^2)	Input	PGA	0	3.92	1.18	1.07	1.15
Factor of safety	Output	FOS	0.783	2.46	1.19	0.35	0.12

Here, PGA was utilized to show the effect of earthquake in horizontal direction on slope stability. It is worth mentioning that all models were designed using the same soil density ($\gamma = 18$ kg/m^3). Hence, soil density was not set as input parameter in modeling of FOS. Table 1 shows the statistical information of input and output parameters used in the networks modeling. The following sections describe modeling procedure of ANN and PSO–ANN techniques.

4.1 Prediction of FOS using ANN

In this study, an attempt was made to predict FOS using ANN technique. To do this, firstly, all 699 datasets were normalized in the range of (0,1) using the following equation:

$$X_{\text{norm}} = (X - X_{\text{min}})/(X_{\text{max}} - X_{\text{min}}) \quad (5)$$

where X is the measured value, X_{norm} represents the normalized value of the measured parameter, X_{min} and X_{max} are the minimum and maximum values of the measured parameters in the dataset. Then, ANN parameters (i.e., momentum coefficient and learning rate) should be determined, since these parameters play an important role in the performance capacity of the network. A brief review of the previous studies is required to determine the values of these parameters. If the selected learning rate is small, the training rate will be slow, because minor changes to weights can be occurred when small values of learning rate are implemented [50, 57]. In addition, fluctuations may happen in the results of training phase caused using large values of learning rate [57, 58]. Different learning rate values have been proposed by several authors. Learning rates of 0.05 and 0.5 were suggested in the studies conducted by Jahed Armaghani et al. [20] and Choobbasti et al. [27], respectively. Yilmaz and Yuksek [59], Erzin and Cetin [29] and Momeni et al. [21] recommended the value of 0.01 for learning rate, while this value was suggested as 0.1 in the study conducted by Yagiz et al. [58]. Apart from learning rate, in the BP algorithm, a steadying effect can be observed by momentum coefficient [60]. Various values have been recommended for momentum coefficient such as 0.95 by Singh et al. [61] and Yagiz et al. [58], 0.9 by Jahed Armaghani et al. [20], 0.0–1.0 by Hassoun [62] and Fu [63] and 0.4–0.9 by Wyhthoff [64].

Table 2 The proposed equations for number of neurons in the hidden layer

Heuristic	References
$\leq 2 \times N_{\text{i}} + 1$	Hecht-Nielsen [67]
$(N_{\text{i}} + N_{\text{o}})/2$	Ripley [72]
$\frac{2+N_{\text{o}}\times N_{\text{i}}+0.5N_{\text{o}}\times(N_{\text{o}}^2+N_{\text{i}})-3}{N_{\text{i}}+N_{\text{o}}}$	Paola [73]
$2N_{\text{i}}/3$	Wang [74]
$\sqrt{N_{\text{i}} \times N_{\text{o}}}$	Masters [75]
$2N_{\text{i}}$	Kaastra and Boyd [76], Kannellopoulas and Wilkinson [66]

N_{i} number of input neuron, N_{o} number of output neuron

According to the above discussion, it seems that different values of learning rates and the momentum coefficients can be utilized to solve the engineering problems. To determine the proper learning rate and momentum coefficient, a series of sensitivity analyses were performed in this study. Considering the provided information by various researchers and the trial-and-error procedure performed in this study, values of 0.05 and 0.9 were chosen for learning rate and the momentum coefficient, respectively.

Besides, performance of ANN models also depends strongly on the architecture of the network as mentioned in the studies by Hush [65] and Kanellopoulas and Wilkinson [66]. Therefore, determination of the optimal architecture is required to design an ANN model. The network architecture is defined as the number of hidden layer(s) and the number of nodes in each hidden layer(s). According to various researchers (e.g., [67–69]) and considering the results of several studies (e.g., [20, 52]), one hidden layer can solve any complex function in a network. Hence, in this study, one hidden layer was chosen to construct the ANN models. In addition, determining neuron number(s) in the hidden layer is the most critical task in the ANN architecture as highlighted by Sonmez et al. [57] and Sonmez and Gokceoglu [70]. Table 2 presents some proposed equations for determination of number of neuron by several scholars. As mentioned earlier, H, α, C, ϕ and PGA were used as model inputs in this study. Based on Table 2, considering 5 neurons in input layer (N_{i}) and one neuron in output layer (N_{o}), the number of neurons which should be used in the

Table 3 R^2 of trained ANN models to predict FOS

Model no.	Nodes in hidden layers	Network result											
		Iteration 1		Iteration 2		Iteration 3		Iteration 4		Iteration 5		Average	
		R^2		R^2		R^2		R^2		R^2		R^2	
		Train	Test	Train	Test	Train	Test	Train	Test	Train	Test	Train	Test
1	1	0.822	0.812	0.843	0.799	0.819	0.833	0.797	0.809	0.828	0.818	0.822	0.814
2	2	0.843	0.802	0.854	0.860	0.809	0.819	0.849	0.837	0.851	0.854	0.841	0.834
3	3	0.844	0.831	0.861	0.815	0.810	0.826	0.845	0.840	0.858	0.852	0.844	0.833
4	4	0.865	0.881	0.872	0.832	0.831	0.808	0.862	0.847	0.860	0.843	0.858	0.842
5	5	0.877	0.821	0.849	0.879	0.852	0.861	0.833	0.870	0.880	0.874	0.858	0.861
6	6	0.882	0.819	0.889	0.845	0.875	0.834	0.868	0.860	0.856	0.866	0.874	0.845
7	7	0.899	0.877	0.887	0.865	0.901	0.876	0.867	0.889	0.89	0.875	0.889	0.876
8	8	0.904	0.888	0.856	0.898	0.907	0.91	0.889	0.901	0.909	0.881	0.893	0.896
9	9	0.911	0.916	0.892	0.907	0.905	0.897	0.913	0.91	0.918	0.911	0.908	0.908
10	10	0.919	0.91	0.921	0.915	0.914	0.899	0.907	0.911	0.92	0.917	0.916	0.910
11	11	0.912	0.915	0.922	0.889	0.909	0.919	0.91	0.92	0.901	0.877	0.911	0.904

Fig. 3 R^2 values of both training and testing datasets for all 11 models

hidden layer is in the range of 1 and 11. It should be noted that $(2\ N_i + 1)$ is the upper limit for the number of hidden layer neurons needed to map any continuous function, as discussed by Caudill [71].

In the next step, all 699 datasets were selected randomly to five different datasets for developing intelligent models. Eventually, a comparison was made to select the most precise one among them. To determine the optimum number of neurons in the hidden layer, using 5 randomly selected datasets, 55 ANN models were constructed using one hidden layer and number of hidden neurons of 1 to 7 as shown in Table 3. Levenberg–Marquardt (LM) learning algorithm was used in constructing ANN models. Study by Hagan and Menhaj [77] suggests the efficiency of this algorithm compared to other conventional gradient descent techniques. Average R^2 values of both training and testing datasets for all 11 models are displayed in Fig. 3. According to this figure, model no. 10 with hidden neurons of 10 outperforms the other models. Hence, 10 was selected as number of hidden neurons in constructing ANN models. It should be noted that only results of R^2 are considered as performance criteria to select the best model. Performance indices of all models with 10 hidden nodes for training and testing datasets are presented in Table 6. More discussion regarding the selection of the best ANN model to predict FOS will be given in "Results and discussion".

4.2 Prediction of FOS using PSO–ANN

A PSO–ANN model performs best when its parameters are properly chosen. A three-layered hybrid of PSO–ANN model was employed to predict FOS values of 699

Table 4 Effects of different numbers of countries in predicting FOS

Model no.	Swarm size	Network result				Ranking				Total rank
		Train		Test		Train		Test		
		R^2	RMSE	R^2	RMSE	R^2	RMSE	R^2	RMSE	
1	25	0.840	0.083	0.867	0.080	1	2	1	3	7
2	50	0.906	0.064	0.908	0.064	2	3	2	4	11
3	75	0.909	0.064	0.914	0.058	3	3	4	5	15
4	100	0.918	0.060	0.910	0.064	4	4	3	4	15
5	150	0.944	0.050	0.934	0.053	7	7	5	6	25
6	200	0.951	0.048	0.940	0.046	9	8	6	8	31
7	250	0.942	0.051	0.954	0.044	6	6	9	9	30
8	300	0.937	0.053	0.957	0.041	5	5	10	10	30
9	350	0.966	0.038	0.964	0.032	12	12	11	12	47
10	400	0.964	0.041	0.965	0.034	11	11	12	11	45
11	450	0.954	0.045	0.942	0.050	10	10	7	7	34
12	500	0.948	0.047	0.951	0.050	8	9	8	7	32

homogenous slopes. As mentioned earlier, several PSO parameters such as number of particles or swarm size and acceleration constants (C_1 and C_2) have an important role in performance capacity of PSO–ANN model. Therefore, a series of sensitivity analyses are required to determine the optimum PSO parameters. A MATLAB code was developed to execute the sensitivity analyses. These analyses consist of several independent steps to determine the optimum number of particles, the maximum number of iteration and acceleration constants. In the following sections, process of developing PSO–ANN predictive model is described.

4.2.1 Swarm size

To determine the optimum number of particles in the swarm (or swarm size), a series of sensitivity analyses were applied to the PSO swarm size in consequence of the fact that there is no method to find the optimum swarm size. While a small swarm may fail to converge to a global solution, choosing a large swarm may lead to delay in the convergence process and decrease efficiency [78]. According to Mendes et al. [79], the size of swarm commonly varies from 20 to 50, but the optimum number depends on the specifications of the problem. Kennedy and Clerc [80] proposed a relationship to determine the optimum swarm size. Based on their relationship, the optimum swarm size depends on the number of variables in each particle. However, Clerc [81] showed that the result of this equation might not always be a good estimator of the optimum swarm size. In the study conducted by Hajihassani et al. [52], swarm size = 275 was selected to predict air-overpressure induced by blasting operation. In addition, swarm size values of 300 and 250 were used in the studies conducted by Jahed Armaghani et al. [53] and Momeni et al. [32], respectively, to solve their problems.

The analyses were conducted using 200 repetitions for each nominee swarm size and fixed values of acceleration constants ($C_1 = C_2 = 2$). Acceleration constants values of 2 were used based on suggestions of Shi and Eberhart [45] and Mendes et al. [79]. Note that, in the modeling of PSO–ANN technique, the other obtained parameters from ANN modeling (e.g., number of hidden node = 10) were set constant. The target of the sensitivity analyses is to find minimum RMSE and maximum R^2 for the network. Table 4 shows the results of sensitivity analyses for training and testing datasets using swarm size in the range of 25–500. The model will be excellent if the R^2 is one and RMSE is zero. As shown in Table 4, generally, increase in swarm size causes increase in R^2 values and decrease in RMSE values. Since selection of the best model is too difficult, a simple ranking method proposed by Zorlu et al. [82] was applied to obtain the optimum swarm size. Results of ranking values for training and testing of each model as well as their total rank values were calculated and shown in Table 4. Value of 47 for total rank shows higher rank value compared to other models. Therefore, swarm size of 350 was selected in predicting FOS in this study.

4.2.2 Termination criteria

The second step of the sensitivity analysis was conducted to determine a termination criterion in the analysis. The termination criteria can be termed as conditions for ending the iterative procedure. For the problem in hand, the maximum number of iterations was considered as termination criterion. In other words, the iterative process was stopped when the number of iterations reached maximum.

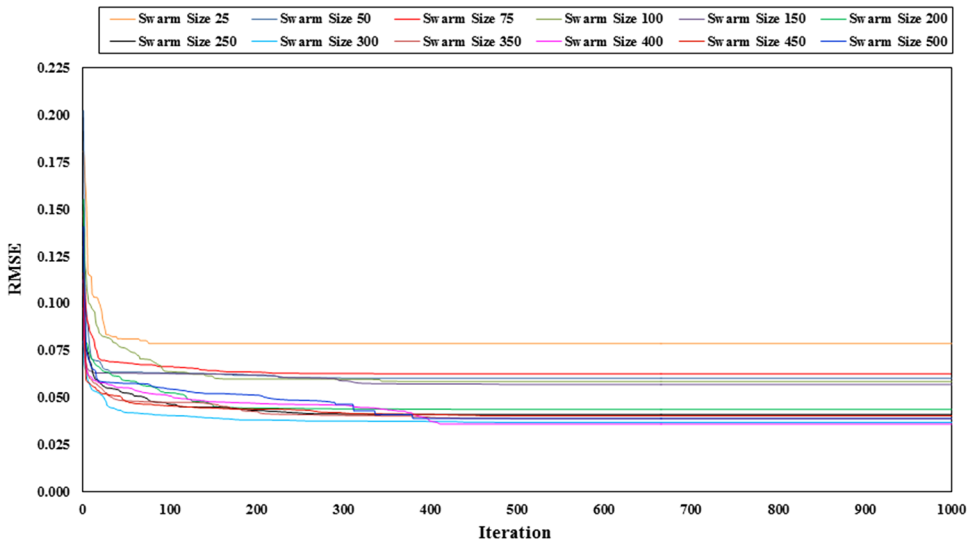

Fig. 4 The effect of the number of iteration on the network performance

Maximum numbers of iterations were obtained as 450 in the study conducted by Tonnizam Mohamad et al. [51] to develop a model for prediction of UCS. In addition, Momeni et al. [32] introduced numbers of iterations = 400 for the same problem. Value of 300 was selected as the maximum number of iterations by Jahed Armaghani et al. [54] to predict shear strength parameters. It should be mentioned that the training time is gradually increased by increasing the maximum number of iteration. Based on the above discussion, there is no common method to achieve the maximum number of iteration. Therefore, a series of sensitivity analyses were applied on PSO–ANN network to find the appropriate number of iteration. These analyses were conducted by setting fixed iteration number of 1,000, the value of 2 for both C_1 and C_2. The target of the sensitivity analyses is to monitor the changes in the cost function (RMSE) in each iteration. Figure 4 shows the results of sensitivity analyses on the iteration number for the swarm size of 25–500 in predicting FOS. According to this figure, the significant changes happened in the first iterations, whereas the changes were moderate up to iteration no. of 400. After iteration number equals to 400, there is no significant change in RMSE, hence this value was selected to be used in simulations. It should be mentioned that in constructing these models, the structure obtained by ANN model ($5 \times 10 \times 1$) was utilized.

4.2.3 Acceleration constants

The next step of sensitivity analysis is to determine the optimum values of acceleration constants (C_1 and C_2). These constants were suggested as 2 for both C_1 and C_2 in the original [43] and modified [83] versions of PSO. The original values ($C_1 = C_2 = 2$) of these coefficients were implemented in several studies [45, 50, 79, 84]. Nevertheless, different values of these constants were also applied to solve various problems. Jahed Armaghani et al. [53] used values of 1 and 1.5 for C_1 and C_2 constants, respectively, to predict flyrock and ground vibration induced by blasting. In another study, $C_1 = 1.333$ and $C_2 = 2.667$ were suggested by Hajihassani et al. [52] to predict air-overpressure resulting from quarry blasting. In addition, values of $C_1 = 1.714$ and $C_2 = 2.286$ were utilized to predict geotechnical complex problems in the studies by Jahed Armaghani et al. [54] and Momeni et al. [32]. With this introduction, it seems that a series of sensitivity analyses are required to select the best constants combination. Different combinations of C_1 and C_2 were applied using PSO parameters obtained from previous steps (swarm size of 350 and iteration number of 400) and also considering suggested structure of ANN modeling part. The results of sensitivity analyses are presented in Table 5. As it can be seen in this table, 12 models were constructed and the related results were presented for training and testing datasets based on R^2 and RMSE. Similar to previous steps of PSO modeling, simple ranking method was used to choose the best combinations. According to total rank values presented in this table, model no. 2 ($C_1 = 1.333$ and $C_2 = 2.667$) outperforms the other models. Therefore, these values were selected as acceleration constants in this study.

4.2.4 Network architecture

In the last step of PSO–ANN modeling, similar to ANN predictive model, network architecture should be determined to train the system. In this study, in order to have a perfect comparison, the same architecture of the ANN modeling should be used. Therefore, the same suggested architecture

Table 5 Effects of different combinations of C_1 and C_2 in predicting FOS

Model no.	C_1	C_2	Network result				Ranking				Total rank
			Train		Test		Train		Test		
			R^2	RMSE	R^2	RMSE	R^2	RMSE	R^2	RMSE	
1	0.8	3.2	0.981	0.030	0.981	0.025	11	11	11	12	45
2	1.333	2.667	0.982	0.029	0.982	0.025	12	12	12	12	48
3	1.714	2.286	0.969	0.035	0.968	0.043	9	9	8	9	35
4	3.2	0.8	0.897	0.069	0.916	0.052	4	4	4	7	19
5	2.667	1.333	0.920	0.060	0.920	0.056	6	5	5	6	22
6	2.286	1.714	0.923	0.057	0.904	0.071	7	8	3	3	21
7	2.5	2.5	0.974	0.034	0.978	0.029	10	10	10	11	41
8	2	2	0.974	0.034	0.975	0.033	10	10	9	10	39
9	1.75	1.75	0.916	0.058	0.921	0.066	5	7	6	4	22
10	1.5	1.5	0.923	0.059	0.897	0.065	7	6	2	5	20
11	1.25	1.25	0.926	0.057	0.942	0.051	8	8	7	8	31
12	1	1	0.853	0.082	0.851	0.075	3	3	1	2	9

Table 6 Performance indices of each model and their rank values in predicting FOS

Method	Model	R^2	RMSE	VAF	Rating for R^2	Rating for RMSE	Rating for VAF	Rank value
ANN	Train 1	0.919	0.062	91.770	3	4	4	11
	Train 2	0.921	0.061	91.903	5	5	5	15
	Train 3	0.914	0.063	91.348	2	3	2	7
	Train 4	0.907	0.065	90.678	1	2	1	4
	Train 5	0.920	0.062	91.683	4	4	3	11
	Test 1	0.910	0.057	90.630	2	4	2	8
	Test 2	0.915	0.057	91.362	4	4	4	12
	Test 3	0.899	0.061	89.321	1	2	1	4
	Test 4	0.911	0.058	90.723	3	3	3	9
	Test 5	0.917	0.055	91.591	5	5	5	15
POS-ANN	Train 1	0.982	0.030	98.126	5	3	4	12
	Train 2	0.982	0.029	98.153	5	4	5	14
	Train 3	0.979	0.030	97.791	3	3	2	8
	Train 4	0.977	0.033	97.594	2	2	1	5
	Train 5	0.981	0.028	98.069	4	5	3	12
	Test 1	0.986	0.022	98.593	5	5	5	15
	Test 2	0.982	0.025	98.184	4	4	4	12
	Test 3	0.979	0.039	97.358	2	2	1	5
	Test 4	0.977	0.029	97.719	1	3	3	7
	Test 5	0.980	0.039	97.397	3	2	2	7

of ANN part (5 × 10 × 1) was performed in PSO–ANN technique to predict FOS. Considering the obtained parameters from previous steps and using the same five randomly selected datasets of ANN part, five PSO–ANN models were constructed. Network performances of these datasets are presented in Table 6. More information regarding the selection of best PSO–ANN model for prediction of FOS will be given in "Results and discussion".

5 Results and discussion

In this research, two intelligent techniques namely ANN and PSO–ANN were developed to predict FOS values of homogenous slopes. During the modeling process of this study, all 699 datasets were randomly divided into 5 different datasets (training and testing) for developing intelligent models. Some performance indices including R^2, value

account for (VAF) and RMSE were computed to check the capacity performance of all the predictive models:

$$R^2 = 1 - \frac{\sum_{i=1}^{N}(y - y')^2}{\sum_{i=1}^{N}(y - \tilde{y})^2} \quad (6)$$

$$\text{VAF} = \left[1 - \frac{\text{var}\,(y - y')}{\text{var}\,(y)}\right] \times 100 \quad (7)$$

$$\text{RMSE} = \sqrt{\frac{1}{N}\sum_{\text{i=1}}^{\text{N}}(y - y')^2} \quad (8)$$

where y, y' and $\tilde{y}$ are the measured, predicted and mean of the y values, respectively, N is the total number of data and P is the number of predictors. Theoretically, the model will be excellent if the R^2 is one, VAF is 100 and RMSE is zero. Results of models performance indices (R^2, RMSE and VAF) for all randomly selected datasets based on training and testing are presented in Table 6.

Table 7 Results of total rank for all predictive techniques obtained from five randomly selected datasets

Method	Model	Total rank
ANN	1	19
	2	27
	3	11
	4	13
	5	26
PSO–ANN	1	27
	2	26
	3	13
	4	12
	5	19

High performances of the training datasets indicate that the learning process of the predictive models is successful if those of testing datasets reveal that the models' generalization ability is satisfactory. As it can be seen in Table 6, selecting the best models is too difficult. To overcome this difficulty, a simple ranking procedure suggested by Zorlu et al. [82] was used to select the best models. A ranking value was calculated and assigned for each training and testing dataset separately (see Table 6). Total ranking of training and testing datasets for two intelligent systems in predicting FOS is shown in Table 7. According to this table, models no. 2 and 1 exhibited the best performances of FOS prediction for ANN and PSO–ANN techniques, respectively. Based on the presented results, considering both training and testing datasets, the prediction performances of the PSO–ANN models are higher than those of ANN models. For more information regarding simple ranking procedure, refer to study conducted by Zorlu et al. [82].

The graphs of predicted FOS using the best ANN and PSO–ANN models against their measured values for training and testing datasets are shown in Figs. 5 and 6, respectively. As shown in these figures, PSO–ANN model can provide higher performance capacity in prediction of FOS in comparison to ANN predictive model. In these figures, R^2 values of testing datasets equal to 0.915 and 0.986 for ANN and PSO–ANN techniques, respectively, suggest the superiority of the PSO–ANN technique in predicting FOS. In addition, RMSE values of 0.057 and 0.022 for testing datasets of ANN and PSO–ANN approaches, respectively, reveal that PSO–ANN can provide higher performance capacity for prediction of FOS compared to ANN. According to these results, although both intelligent techniques can predict FOS with high level of accuracy, PSO–ANN can be used when more accurate results are required.

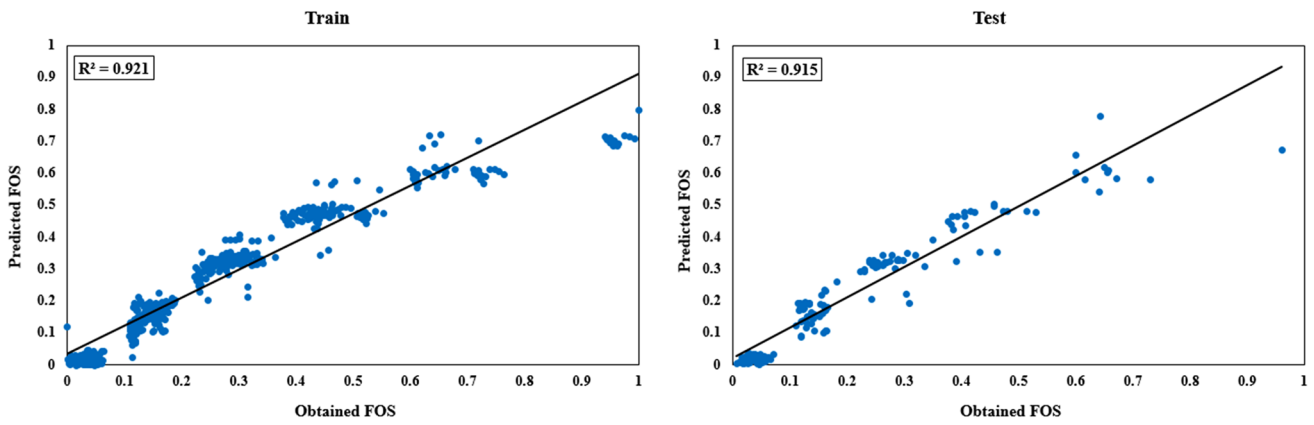

Fig. 5 R^2 of obtained and predicted values of FOS for the best model of ANN

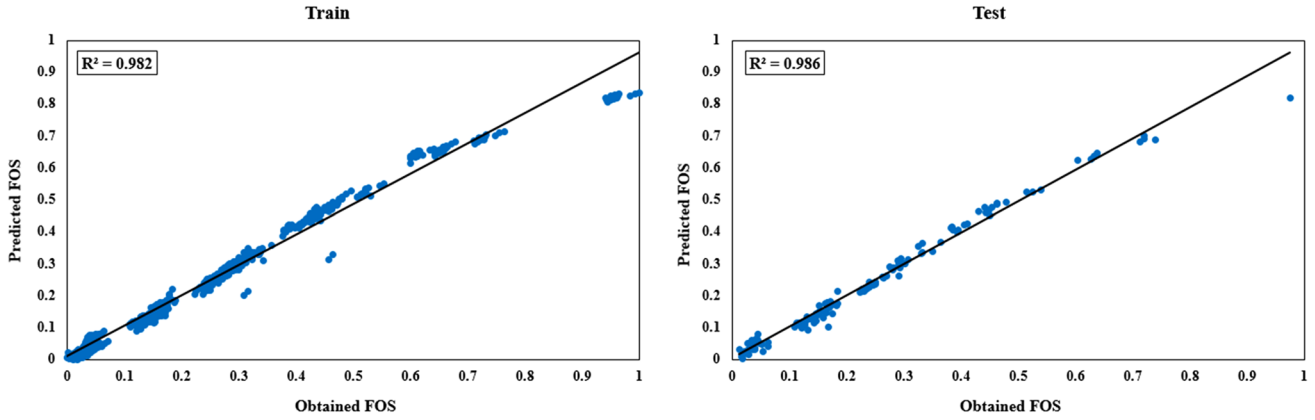

Fig. 6 R^2 of obtained and predicted values of FOS for the best model of PSO–ANN

6 Conclusion

To prepare an appropriate database for developing two intelligent systems namely ANN and PSO–ANN to predict FOS, a series of seismic analyses were conducted on 699 of homogeneous slopes (in terms of material) using Geostudio software. For this purpose, the most influential parameters on slope stability including slope height, gradient, cohesion, friction angle and PGA were considered as model inputs. In modeling procedure of intelligent systems, all 699 datasets were randomly selected to 5 different datasets (training and testing). Considering some model performance indices such as RMSE and VAF and using simple ranking method proposed by Zorlu et al. [82], the best models were selected among all constructed models of ANN and PSO–ANN. The results indicated that the PSO–ANN technique can provide higher performance capacities in predicting FOS. R^2 values of testing datastets equal to 0.915 and 0.986 for ANN and PSO–ANN techniques, respectively, suggest the superiority of the PSO–ANN technique. Although all proposed models in this study are applicable for FOS prediction, they can be used depending on the conditions. When higher accuracy of FOS is required, PSO–ANN model would be the proper alternative as it can optimize the weights and biases of the network connection for training by ANN.

References

1. Bishop AW (1955) The use of the slip circle in the stability analysis of slopes. Institution of civil engineers
2. Spencer E (1967) A method of analysis of the stability of embankments assuming parallel inter-slice forces. Geotechnique 17:11–26
3. Morgenstern NR, Price VE (1965) The analysis of the stability of general slip surfaces. Geotechnique 15:79–93
4. Sarma SK (1973) Stability analysis of embankments and slopes. Geotechnique 23(3):423–433
5. Sarma SK (1979) Stability analysis of embankments and slopes. J Geotech Eng Division 105(12):1511–1524
6. Baker R (2006) A relation between safety factors with respect to strength and height of slopes. Comput Geotech 33(4):275–277
7. Huang M, Jia CQ (2009) Strength reduction FEM in stability analysis of soil slopes subjected to transient unsaturated seepage. Comput Geotech 36(1):93–101
8. El-Ramly H, Morgenstern NR, Cruden DM (2002) Probabilistic slope stability analysis for practice. Can Geotech J 39(3):665–683
9. Tobutt DC (1982) Monte Carlo simulation methods for slope stability. Comput Geosci 8(2):199–208
10. Wang JP, Huang D (2012) RosenPoint: a Microsoft Excel-based program for the Rosenblueth point estimate method and an application in slope stability analysis. Comput Geosci 48:239–243
11. Lee S, Pradhan B (2006) Probabilistic landslide risk mapping at Penang Island, Malaysia. J Earth Syst Sci 115(6):661–672
12. Irigaray C, El Hamdouni R, Jiménez-Perálvarez JD, Fernández P, Chacón J (2012) Spatial stability of slope cuts in rock massifs using GIS technology and probabilistic analysis. Bull Eng Geol Environ 71:569–578
13. Lee S, Pradhan B (2007) Landslide hazard mapping at Selangor, Malaysia using frequency ratio and logistic regression models. Landslides 4:33–41
14. Kanungo DP, Arora MK, Sarkar S, Gupta RP (2006) A comparative study of conventional. ANN black box, fuzzy and combined neural and fuzzy weighting procedures for landslide susceptibility zonation in Darjeeling Himalayas, EngGeol 85:347–366
15. Yilmaz I (2009) A case study from Koyulhisar (Sivas-Turkey) for landslide susceptibility mapping by artificial neural networks. Bull Eng Geol Environ 68:297–306
16. Oh HJ, Pradhan B (2011) Application of a neuro-fuzzy model to landslide susceptiblity mapping for shallow landslides in tropical hilly area. Comput Geosci 37:1264–1276
17. Rezaei M, Monjezi M, Yazdian Varjani A (2011) Development of a fuzzy model to predict flyrock in surface mining. Safety Sci 49:298–305
18. Khandelwal M, Kumar DL, Yellishetty M (2011) Application of soft computing to predict blast-induced ground vibration. Eng Comput 27(2):117–125
19. Bahrami A, Monjezi M, Goshtasbi K, Ghazvinian A (2011) Prediction of rock fragmentation due to blasting using artificial neural network. Eng Comput 27(2):177–181
20. Jahed Armaghani D, Tonnizam Mohamad E, Momeni E, Narayanasamy MS, Mohd Amin MF (2014) An adaptive neuro-fuzzy inference system for predicting unconfined compressive strength

and Young's modulus: a study on Main Range granite. Bull Eng Geol Environ. doi:10.1007/s10064-014-0687-4
21. Momeni E, Nazir R, Armaghani DJ, Maizir H (2014) Prediction of pile bearing capacity using a hybrid genetic algorithm-based ANN. Measurement 57:122–131
22. Tonnizam Mohamad E, Jahed Armaghani D, Hajihassani M, Faizi K, Marto A (2013) A simulation approach to predict blasting-induced flyrock and size of thrown rocks. Electron J Geotech Eng 18:365–374
23. Tonnizam Mohamad E, Noorani SA, Jahed Armaghani D, Saad R (2012) Simulation of blasting induced ground vibration by using artificial neural network. Electron J Geotech Eng 17:2571–2584
24. Sakellariou M, Ferentinou M (2005) A study of slope stability prediction using neural networks. Geotech Geol Eng 24(3):419–445
25. Das SK, Biswal RK, Sivakugan N, Das B (2011) Classification of slopes and prediction of factor of safety using differential evolution neural networks. Environ Earth Sci 64(1):201–210
26. Sah NK, Sheorey PR, Upadhyama LW (1994) Maximum likelihood estimation of slope stability. Int J Rock Mech Min Sci 31:47–53
27. Choobbasti AJ, Farrokhzad F, Barari A (2009) Prediction of slope stability using artificial neural network (case study: Noabad, Mazandaran, Iran). Arab J Geosci 2(4):311–319
28. Samui P, Kothari DP (2011) Utilization of a least square support vector machine (LSSVM) for slope stability analysis. Scientia Iranica 18(1):53–58
29. Erzin Y, Cetin T (2013) The prediction of the critical factor of safety of homogeneous finite slopes using neural networks and multiple regressions. Comput Geosci 51:305–313
30. Adhikari R, Agrawal RK (2011) Effectiveness of PSO based neural network for seasonal time series forecasting. In: Proceedings of the indian international conference on artificial intelligence (IICAI), Tumkur, India, pp 232–244
31. Eberhart RC, Shi Y (2001) Particle swarm optimization: developments, applications and resources. In: Proceedings of IEEE international conference on evolutionary computation, pp 81–86
32. Momeni E, Jahed Armaghani D, Hajihassani M, Amin MFM (2015) Prediction of uniaxial compressive strength of rock samples using hybrid particle swarm optimization-based artificial neural networks. Measurement 60:50–63
33. Yu Y, Xie L, Zhang B (2005) Stability of earth–rockfill dams: influence of geometry on the three-dimensional effect. Comput Geotech 32(5):326–339
34. Kramer SL (1996) Geotechnical earthquake engineering. Prentice-Hall, New Jersey
35. Dreyfus G (2005) Neural Networks: methodology and application. Springer, Berlin
36. Monjezi M, Khoshalan HA, Varjani AY (2012) Prediction of flyrock and backbreak in open pit blasting operation: a neuro-genetic approach. Arab J Geosci 5(3):441–448
37. Maulenkamp F, Grima MA (1999) Application of neural networks for prediction of the unconfined compressive strength (UCS) from Equotip Hardness. Int J Rock Mech Min Sci 36:29–39
38. Tonnizam Mohamad E, Hajihassani M, Jahed Armaghani D, Marto A (2012) Simulation of blasting-induced air overpressure by means of artificial neural networks. Int Rev Model Simul 5(6):2501–2506
39. Marto A, Hajihassani M, JahedArmaghani D, Tonnizam Mohamad E, Makhtar AM (2014) A novel approach for blast-induced flyrock prediction based on imperialist competitive algorithm and artificial neural network. Sci World J, Article ID 643715
40. Monjezi M, Ahmadi Z, Varjani AY, Khandelwal M (2013) Back-break prediction in the Chadormalu iron mine using artificial neural network. Neural ComputAppl 23:1101–1107
41. Kosko B (1994) Neural networks and fuzzy systems: a dynamical systems approach to machine intelligence. Prentice Hall, New Delhi
42. Simpson PK (1990) Artificial neural system: foundation, paradigms, applications and implementations. Pergamon, New York
43. Kennedy J, Eberhart RC (1995) Particle swarm optimization. In: Proceedings of IEEE international conference on neural networks, Piscataway, pp 1942–1948
44. Poli R, Kennedy J, Blackwell T (2007) Particle swarm optimization. Swarm Intell 1(1):33–57
45. Shi Y, Eberhart RC (1999) Empirical study of particle swarm optimization. In: Proceedings of evolutionary computation, CEC, Proceedings of the 1999 Congress, IEEE
46. Das MT, Dulger LC (2009) Signature verification (SV) toolbox: application of PSO-NN. Eng Appl Artif Intel 22(4):688–694
47. Victoire T, Jeyakumar AE (2004) Hybrid PSO–SQP for economic dispatch with valve-point effect. Electr Pow Syst Res 71(1):51–59
48. Ismail A, Jeng DS, Zhang LL (2013) Anoptimised product-unit neural network with a novel PSO–BP hybrid training algorithm: applications to load–deformation analysis of axially loaded piles. Eng Appl Artif Intel 26(10):2305–2314
49. Zhang JR, Zhang J, Lok TM, Lyu MR (2007) A hybrid particle swarm optimization–back-propagation algorithm for feedforward neural network training. Appl Math Comput 185(2):1026–1037
50. Engelbrecht AP (2007) Computational intelligence: an introduction, 2nd edn. Wiley, New York
51. Tonnizam Mohamad E, Jahed Armaghani D, Momeni E, Abad SVANK (2014) Prediction of the unconfined compressive strength of soft rocks: a PSO-based ANN approach. Bull Eng Geol Environ. doi:10.1007/s10064-014-0638-0
52. Hajihassani M, JahedArmaghani D, Sohaei H, Tonnizam Mohamad E, Marto A (2014) Prediction of airblast-overpressure induced by blasting using a hybrid artificial neural network and particle swarm optimization. Appl Acoust 80:57–67
53. JahedArmaghani D, Hajihassani M, Tonnizam Mohamad E, Marto A, Noorani SA (2013) Blasting-induced flyrock and ground vibration prediction through an expert artificial neural network based on particle swarm optimization. Arab J Geosci. doi:10.1007/s12517-013-1174-0
54. JahedArmaghani D, Hajihassani M, Yazdani Bejarbaneh B, Marto A, Tonnizam Mohamad E (2014) Indirect measure of shale shear strength parameters by means of rock index tests through an optimized artificial neural network. Measurement 55:487–498
55. Montana DJ, Davis L (1989) Training feedforward neural networks using genetic algorithms. IJCAI 89:762–767
56. Socha K, Blum C (2007) An ant colony optimization algorithm for continuous optimization: application to feed-forward neural network training. Neural ComputAppl 16:235–247
57. Sonmez H, Gokceoglu C, Nefeslioglu HA, Kayabasi A (2006) Estimation of rock modulus: for intact rocks with an artificial neural network and for rock masses with a new empirical equation. Int J Rock Mech Min Sci 43:224–235
58. Yagiz S, Gokceoglu C, Sezer E, Iplikci S (2009) Application of two non-linear prediction tools to the estimation of tunnel boring machine performance. Eng Appl Artif Intel 22(4):808–814
59. Yilmaz I, Yuksek G (2009) Prediction of the strength and elasticity modulus of gypsum using multiple regression, ANN, and ANFIS models. Int J Rock Mech Min Sci 46(4):803–810
60. Negnevitsky M (2002) Artificial Intelligence: A Guide to Intelligent Systems. Addison-Wesley, England
61. Singh VK, Singh D, Singh TN (2001) Prediction of strength properties of some schistose rocks from petrographic properties using artificial neural networks. Int J Rock Mech Min Sci 38(2):269–284
62. Hassoun MH (1995) Fundamentals of Artificial Neural Networks. MIT Press, Cambridge

63. Fu L (1995) Neural networks in computer intelligence. McGraw-Hill, New York
64. Wyhthoff BJ (1993) Backpropagation neural networks: a tutorial. Chemometr Intell Lab Syst 18:115–155
65. Hush DR (1989) Classification with neural networks: a performance analysis. In: Proceedings of the IEEE international conference on systems engineering. Dayton, OH, USA, pp 277–280
66. Kanellopoulas I, Wilkinson GG (1997) Strategies and best practice for neural network image classification. Int J Remote Sens 18:711–725
67. Hecht-Nielsen R (1987) Kolmogorov's mapping neural network existence theorem. In: Proceedings of the First IEEE international conference on neural networks, San Diego, CA, USA, pp 11–14
68. Hornik K, Stinchcombe M, White H (1989) Multilayer feedforward networks are universal approximators. Neural Netw 2:359–366
69. Baheer I (2000) Selection of methodology for modeling hysteresis behavior of soils using neural networks. J Comput Aid Civil Infrastruct Eng 5(6):445–463
70. Sonmez H, Gokceoglu C (2008) Discussion on the paper by H. Gullu and E. Ercelebi A neural network approach for attenuation relationships: an application using strong ground motion data from Turkey. Eng Geol 97:91–93
71. Caudill M (1988) Neural networks primer part III. Al Expert 3(6):53–59
72. Ripley BD (1993) Statistical aspects of neural networks. In: Jensen JL, Kendall WS (eds) Barndoff-Neilsen OE networks and chaos-statistical and probabilistic aspects. Chapman & Hall, London, pp 40–123
73. Paola JD (1994) Neural network classification of multispectral imagery. MSc thesis, The University of Arizona, USA
74. Wang C (1994) A theory of generalization in learning machines with neural application. PhD thesis, The University of Pennsylvania, USA
75. Masters T (1994) Practical neural network recipes in C++. Academic Press, Boston
76. Kaastra I, Boyd M (1996) Designing a neural network for forecasting financial and economic time series. Neurocomputing 10:215–236
77. Hagan MT, Menhaj MB (1994) Training feed forward networks with the Marquardt algorithm. IEEE Trans Neural Netw 5(6):861–867
78. Hajihassani M (2013). Tunneling-induced ground movement and building damage prediction using hybrid artificial neural networks. PhD Thesis, Universiti Teknologi Malaysia
79. Mendes R, Cortes P, Rocha M, Neves J (2002) Particle swarms for feed forward neural net training. In: Proceedings of IEEE international joint conference on neural networks, Honolulu, HI, USA, 12–17 May 2002, pp 1895–1899
80. Kennedy J, Clerc M (2006) Standard PSO 2006. http://www.particleswarm.info/Standard-PSO-2006.c
81. Clerc M (2011) Standard particle swarm optimisation, from 2006 to 2011. http://clerc.maurice.free.fr/pso/SPSO_descriptions.pdf (2011-07-13 version)
82. Zorlu K, Gokceoglu C, Ocakoglu F, Nefeslioglu HA, Acikalin S (2008) Prediction of uniaxial compressive strength of sandstones using petrography-based models. Eng Geol 96(3):141–158
83. Clerc M, Kennedy J (2002) The particle swarm explosion, stability, and convergence in a multi-dimensional complex space. IEEE Trans Evol Comput 6:58–73
84. Kalatehjari R, Ali N, Kholghifard M, Hajihassani M (2014) The effects of method of generating circular slip surfaces on determining the critical slip surface by particle swarm optimization. Arab J Geosci 7(4):1529–1539